# Study of the physical properties of CdTe (200): synthesized nanoparticles and grown thin films

Scientific research paper

Marjan Kamalian[*], Lida Babazadeh Habashi, Maryam Gholizadeh Arashti, Ebrahim Hasani

*Department of Physics, Faculty of Science, Yadegar-e-Imam Khomeini (RAH) Shahr-e-Rey Branch, Islamic Azad University, Tehran, Iran*

**ABSTRACT**

In this work, cadmium telluride nanoparticles (CdTe NPs) were synthesized by the sonochemical method; then thin films with thicknesses about 100 nm were deposited on glass substrates using the thermal evaporation technique at substrate temperature of 200 °C and vacuum pressure of $2 \times 10^{-5}$ mbar. The Sonochemical method is one of the best methods for synthesizing nanomaterials with very small particle sizes. After synthesis and deposition, the prepared films were subjected to x-ray diffraction (XRD), ultraviolet-visible (UV-Vis) spectroscopy, and scanning electron microscopy (SEM) to study the structure, optical properties, and morphology of the films. XRD patterns indicated that the grown films were polycrystalline with a cubic structure on the preferred orientation (200). The size of the synthesized nanoparticles and crystallite size of the thin film grown on glass in the preferred orientation (200) were 16 nm and 10.65 nm, respectively. Light absorbance spectra of nanoparticles and the thin film obtained by UV-Vis spectroscopy at the wavelength range 600-1600 nm showed the increase of light absorption after deposition. The optical energy band gap was also increased from 1.48 eV for nanoparticles to 1.51 eV for the deposited films. Further the SEM images taken on the scale of 500 nm from nanoparticles and thin films showed homogeneity and uniformity of both of them.

## 1 Introduction

Semiconductor thin films have been widely used in the recent decades to manufacture many electronic and electro-optical devices such as detectors, nanosensors, photocatalysts, transistors, light emitting diodes, and p-n junctions in solar cells [1- 6]. Among these semiconductors, cadmium telluride (CdTe), which belongs to the II-IV group, has been recently of special importance to researchers due to its cheapness and the variety of synthesis and manufacturing methods. Suitable optical properties of cadmium telluride, including high absorption coefficient ($> 10^5$) and ideal optical energy band gap (about 1.5 eV), make it an adsorbent layer in the second generation of cadmium telluride-based solar cells. The performance of solar cells depends on the proper selection of some parameters during deposition (substrate material, film thickness, temperature and pressure during deposition, velocity and duration of deposition, etc.) [7-9].

The optical properties of films change after deposition by applying certain conditions to the film, such as reannealing in air, vacuum, or some gases (argon) [10-12]. This is carried out under a pressure much higher than atmospheric pressure or bombardment with

gamma nuclei, etc., leading to an increase in the adsorption coefficient of the cadmium telluride thin film as the adsorbent layer. First Solar Company has declared the efficiency of solar cells based on the p-n junction of cadmium telluride and cadmium sulfide (CdS) to be 22.1% [13]. In this junction, cadmium sulfide is a film called window, the thickness of which should be less than 200 nm; by adjusting the cadmium telluride layer, the efficiency of the solar cell can be increased. Also, the high atomic number of cadmium telluride proves the effective use of this substance in the construction of nuclear detectors [14].

Cadmium telluride nanoparticles can be synthesized by various methods such as sol-gel [15], sonochemical method [16], electrochemical precipitation [17], and laser evaporation [18]. Sonochemistry is one of the best methods for synthesizing nanomaterials, producing nanoparticles with very small, uniform and high-quality sizes. In this method, ultrasonic radiation (between 20 kHz and 10 MHz) is applied to the molecules to increase their chemical reactions [19]. The controllability, safety and high speed of reactions in the sonochemical method have led to the development of other synthesis methods based on this method; these are such as ultrasonic sol-gel, sonoelectrochemistry, and ultrasonic laser evaporation [20-21].

Cadmium telluride thin films can be prepared in many ways, the most common of which are thermal evaporation, sputtering, pulsed laser (PLD), electron beam evaporation, rotational deposition, and molecular beam (MBE) [22 -26]. Thermal evaporation is one of the best and most cost-effective deposition methods for making thin films with desired thicknesses on the substrates. In this method, the evaporated particles move at a high speed and in a direct path toward the substrate; as the loss of particles and the possibility of oxide formation on the substrate are minimized, the fabricated layers have the highest quality [27].
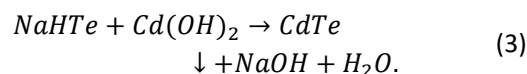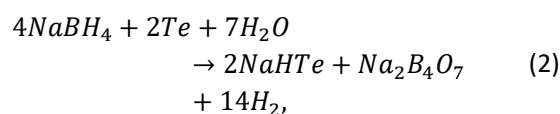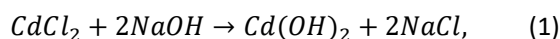
Almost all previous works have investigated the physical properties of CdTe (111) thin films [28-31]. The growth of CdTe thin films with preferred orientations (100) and (001) was studied in recent years [32, 33]. However, deposition of the CdTe (100) on GaAs (100) substrates was reported in the 80s [34, 35]. In the present work, (200)-oriented CdTe NPs are synthesized using the sonochemical method and deposited on the glass substrate using the thermal evaporation method. Then the structural, optical and morphological properties of CdTe (200) were studied.

## 2 Experimental details

### 2.1 Synthesis of nanoparticles

For the synthesis of cadmium telluride nanoparticles by the sonochemical method, 2 g of 99.99% pure cadmium chloride powder ($CdCl2$) (prepared by Sigma Aldrich) was poured into 1 M sodium hydroxide solution (NaOH) to form cadmium hydroxide precipitate, $Cd(OH)_2$ (Eq. (1)). On the other hand, 3 g of tetrahydro borate powder (NaBH4) with the purity of more than 98% (prepared by Sigma Aldrich) was reacted with 1 g of pure tellurium powder (purity above 99.8%, Sigma Aldrich); this was done in 100 ml of distilled water in an ice bath under ultrasonic irradiation for 4 to 5 hours to produce sodium hydrogen tellurium (NaHTe) (Eq. (2)).The resulting product, $Cd(OH)_2$, from Eq. (1) is then reacted with the NaHTe from Eq. (2) to yield a black precipitate of cadmium telluride. After cleaning the material with distilled water and ethanol and drying it for 5 hours at 70 ° C, cadmium telluride nanoparticles are synthesized.

$$CdCl_2 + 2NaOH \rightarrow Cd(OH)_2 + 2NaCl, \qquad (1)$$

$$\begin{aligned} 4NaBH_4 + 2Te + 7H_2O \\ \rightarrow 2NaHTe + Na_2B_4O_7 \\ + 14H_2, \end{aligned} \qquad (2)$$

$$\begin{aligned} NaHTe + Cd(OH)_2 \rightarrow CdTe \\ \downarrow + NaOH + H_2O. \end{aligned} \qquad (3)$$

### 2.2 Thin Film Preparation

The nanoparticles synthesized by sonochemistry were placed in a deposition chamber on a molybdenum flatboat so that after applying the appropriate voltage, the evaporated cadmium telluride nanoparticles could be placed on the substrates by a holder at a distance of about 25 cm from the plant to be deposited. Before the deposition process, the glass substrates were carefully washed with acetone and distilled water for 10 minutes and then dried. The deposition process was performed by thermal evaporation at the pressure of 2×10-5 mbar and temperature of 100 ° C for 30 minutes. By applying the electric current of 100 A and power of 1000 W, the evaporated cadmium telluride nanoparticles were

deposited at a rate of 1 A°/ s on the substrates. The thickness of the prepared films was controlled using a quartz crystal monitor placed just below the substrate holder. Light interferometry also measured the thin film thickness of 100 nm.

## 2.3 Characterization

Diffraction patterns of the synthesized nanoparticles and thin films made of cadmium telluride were obtained by X-ray diffractometer (XRD) (model X'Pert PRO MPD, made by PANalytical, Netherlands), in which the radiation of copper with the wavelength of 1.54060 Å was used and the data were characterized in the range 2θ, 20 ° to 80 ° with a step size of 0.026 ° min-1. Light absorption spectra from nanoparticles and cadmium telluride thin films were prepared using UV-Vis (model Lambda 25, manufactured by Parkin Elmer, USA) in the wavelength range of 600-1600 nm and at room temperature. High-resolution micrographs at 500 nm scale were then taken from the nanoparticles mass and thin film surface to study their morphology using Field Emission Scanning Electron Microscope (FE-SEM) (Model 3 MIRA, manufactured by TE-SCAN, Czech Republic).

## 3 Results and discussion

### 3.1 Structural analysis

XRD diffraction patterns of the synthesized nanoparticles and cadmium telluride thin films were analyzed using X 'Pert High Score software and the phase of each of the peaks formed by matching the obtained patterns was identified according to the ICCD reference diffraction pattern. Figure 1a shows the XRD pattern of nanoparticles and cadmium telluride thin films. The diffraction patterns obtained from nanoparticles showed that the nanoparticles synthesized in this work by the sonochemical method had a cubic structure; unlike the samples synthesized in the previous works [36], the main peak of the diffraction pattern was at an angular position of 2θ=27.61°, which corresponded to the direction (200).

Other peaks could be seen in the nanoparticle diffraction pattern, which were in angular positions at 38.56 °, 49.59 °, 57.07 °, 65.61 °, and 72.06 ° according to the orientations (220), (222), (400), (420) and (422), respectively. The results obtained from this diffraction

pattern were in a good agreement with the JCPDS reference card number 75-2083. In addition to the peaks of cadmium telluride nanoparticles, the presence of two small peaks in the diffraction pattern indicated the formation of $CdTe_2O_5$ during synthesis. The diffraction pattern of cadmium telluride thin film grown on glass, thus, showed that the prepared layer was polycrystalline and its crystalline structure was cubic.

The main peak of the thin film diffraction was prepared according to the preferential orientation (200) at 2θ=27.81°. The other peaks were in angular positions at 39.16, 49.66 °, and 65.69 °, which were, respectively, in the (220), (222), and (420) orientations. As shown in Figure 1a, the peaks formed in thin film diffraction were wider and less intense than nanoparticles, which could be due to the change in the crystal structure of cadmium telluride after deposition. The strain created between cadmium telluride nanoparticles and the glass substrate led to a change in the angular position of the diffraction peaks in the prepared thin film [37]. The removal of $CdTeO_5$ peaks in the thin film diffraction pattern could also be done by thermal evaporation when the material is deposited, which generally produces films without oxidation.

The average nanoparticle size and crystallinity of the thin film D, dislocation density δ, microstrain ε, and texture coefficient $T_c$, of the film are obtained from Debye-Scherrer, Williamson-Smallman, Hall and Harris relations, respectively [38-41].

$$D = \frac{0.94\lambda}{B \cos \theta}, \qquad (4)$$

$$B \cos \theta = \varepsilon \sin \theta + \frac{\lambda}{D} \qquad (5)$$

$$\delta = \left(\frac{1}{D^2}\right), \qquad (6)$$

$$T_c(hkl) = \left(\frac{\frac{I(hkl)}{I_0(hkl)}}{\frac{1}{N}\sum_N \frac{I(hkl)}{I_0(hkl)}}\right), \qquad (7)$$

where B is the full width at half maximum (FWHM). The θ is the Bragg's angle, I (hkl) is the measured intensity of each peak, $I_0$ (hkl) is the reference intensity of the same peak in JCPDS, and N is the number of peaks observed. The results of XRD analysis are given

in Table 1. The size of nanoparticles synthesized was almost the same in all crystal plates, thus indicating the uniformity and homogeneity of nanoparticles synthesized by the sonochemical method. Also, the reduction in the crystalline size of the thin films grown on the glass substrate, when compared to the size of the synthesized nanoparticles, which was due to the diffusion of diffraction peaks (increase of FWHM) in different directions, could be attributed to the change in the polycrystalline structure of the films after deposition by the thermal evaporation method.

The lattice parameter values (a) of the crystal structure in different directions for the nanoparticles and the thin film are calculated from the equation and shown in Figure 1b,

$$a = d_{hkl}\sqrt{h^2 + k^2 + l^2}, \qquad (8)$$

where (hkl) are Miller indices. The lattice parameter obtained for cadmium telluride nanoparticles in the (200) direction is greater than its value for the reference cadmium telluride nanoparticles (6.410 A°), thus indicating the compressive strain created in the synthesized nanoparticles. After deposition, the lattice parameter decreases in all crystalline plates, showing tensile stress in the thin film due to the mismatch between the lattices of cadmium telluride nanoparticles and the substrates.

A slight increase in the microstrain of the grown layers, as shown in Figure 1c, relative to the synthesized nanoparticles, indicated a slight deviation from the ideal crystallinity of the nanoparticles, leading to a decrease in the crystalline size of the grown films. Quantitative information about the orientations and the share of each of the selected reflective directions, in comparison with the random orientations in nanoparticles and thin films, could be obtained by calculating the texture coefficient $T_C$, from Eq. (7). Values higher than 1 for each orientation indicate the tendency of the material to choose that direction [42]. In the synthesized nanoparticles, the texture coefficient for the direction (200) was the highest value, thus confirming the selection of the direction (200) as the preferred orientation of nanoparticles. $T_C$ of (200) orientation of deposited film still has the highest value, indicating that the preferred orientation does not change during the deposition process.

Table 1. Results of the XRD pattern analysis of cadmium telluride thin film.

| Material | angle (2θ) | Crystallite size (nm) | Microstrain (×10⁻³) |
|---|---|---|---|
| nanoparticle | 27.61 | 16.57 | 2.34 |
| | 36.56 | 10.96 | 2.55 |
| | 49.59 | 14.50 | 1.52 |
| | 57.07 | 16.49 | 1.18 |
| | 65.60 | 14.35 | 1.19 |
| | 72.06 | 17.90 | 0.88 |
| Thin film | 27.81 | 10.65 | 3.65 |
| | 39.16 | 10.25 | 2.69 |
| | 49.66 | 9.98 | 2.20 |
| | 65.69 | 7.49 | 2.30 |

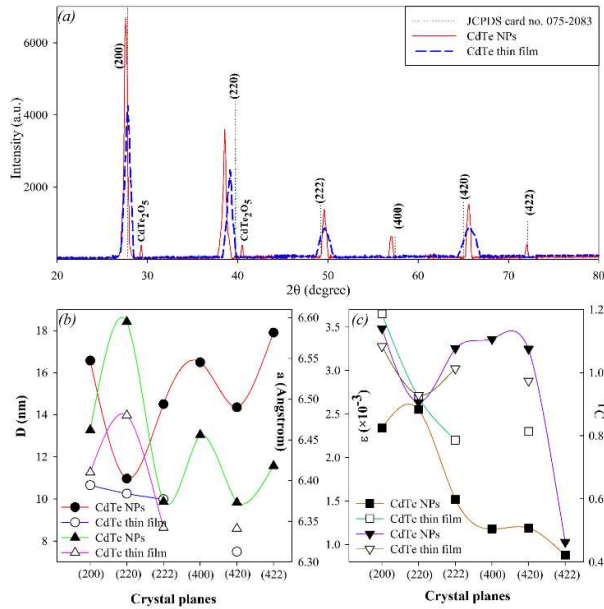| Material) | Dislocation density (×1015) | Lattice parameter (Å) | Texture coefficient |
|---|---|---|---|
| Nanoparticle | 3.64 | 6.462 | 1.140 |
| | 8.32 | 6.595 | 0.906 |
| | 4.75 | 6.374 | 1.077 |
| | 3.68 | 6.456 | 1.106 |
| | 4.86 | 6.373 | 1.075 |
| | 3.12 | 6.418 | 0.463 |
| Thin films | 8.82 | 6.410 | 1.083 |
| | 9.52 | 6.480 | 0.929 |
| | 10.00 | 6.342 | 1.013 |
| | 17.81 | 6.341 | 0.974 |

Figure 1. a) XRD diffraction pattern of synthesized nanoparticles and cadmium telluride thin film. b) Changes in grain size D (hollow and solid circles) and lattice parameter a, (hollow and solid upward triangles) in terms of crystal plates; and c) Microstrain changes ε, (hollow and solid squares) and texture coefficient $T_C$, (hollow and solid downward triangles) in terms of crystalline plates.

## 3.2 Optical properties

The optical absorbance and transmittance spectrum of light by the synthesized nanoparticles and the grown thin film of cadmium telluride was obtained using an ultraviolet-visible optical spectrometer in the wavelength range of 600-1600 nm at room temperature, as shown in Figure 2a. By calculating the logarithm $I_0 / I$, the absorption value (A) could be obtained by the nanoparticles surface and the thin layer, where $I_0$ is the intensity of the incident light and I is the intensity of the light passing through the surfaces.

As can be seen, with increasing the wavelength ($\lambda$ <800 nm), the amount of light absorption reaches its lowest value; then it is almost constant. The decrease in the amount of light absorption by the grown films, as compared to the synthesized nanoparticles, is due to the decrease in the crystalline size and the increase in the grain borders, as well as the thin thickness of the grown films on the glass [43]. In the infrared region, with increasing the wavelength, a greater decrease in the amount of light absorption by the grown thin layer is

observed, this indicated the transparency of the cadmium telluride thin film in this region.

In the wavelength range of 600-700 nm, light absorption by the thin film is higher than that by nanoparticles, thus indicating that the cadmium telluride thin film is adsorbent [44]. The energy band gap of the nanoparticles and the grown films of cadmium telluride is obtained using the linear slope extrusion of the Tauc diagram resulting according to the following equation, as plotted in Figure 2b [45].

$$(\alpha h\nu)^n = C\left(h\nu - E_g\right), \qquad (9)$$

where α is the coefficient of light absorption by the material with the thickness d, which is calculated from Beer-Lambert-Bouguer law [46],

$$\alpha = \frac{2.303\ A}{d}. \qquad (10)$$

Here, $E_g$ is the optical energy band gap and C is a constant value that depends on the mobility of the charge and its value is in the range of $10^8$-$10^7$ m$^{-1}$. For semiconductors such as cadmium telluride that have a direct energy band gap, the value of n is equal to 2. The energy band gap of the synthesized nanoparticles and the grown thin films obtained from Eq. (8) is equal to 1.48 eV and 1.51 eV, respectively, which is consistent with the previous reports [47].

The increase in the energy gap of the grown thin film, as compared to the synthesized nanoparticles, is due to the shift of the adsorption edge in the grown films to the shorter wavelengths, which could be attributed to the strain caused by the mismatch of cadmium telluride nanoparticles and glass substrate [48]. The optical parameters of the extinction coefficient (k) and refractive index (n) of the nanoparticles and the thin film could be obtained from the following equations [47]; they are plotted in Figure 3b in terms of wavelength and photon energy, respectively.

$$k = \alpha\ \frac{\lambda}{4\pi}, \qquad (11)$$

$$n = \left[(1+R) + \{(1+R)^2 - (1-R)^2(1 + k)^2\}^{\frac{1}{2}}\right]/(1-R), \qquad (12)$$

where λ is the wavelength and R is the reflectance of the CdTe surface plotted in Figure 3a and calculated from the following equation [49].

$$R = 1 - (T / \exp(-A))^{0.5}. \qquad (13)$$

Here T is the percentage of light passing through matter. Determining the extinction coefficient is of special importance for calculating the concentration of nanoparticles accumulated on the film. In nanoparticle deposition, which leads to the formation of thin films with a small crystalline size, the extinction coefficient will be dependent on the particle size [50]. For synthesized nanoparticles, the extinction coefficient first decreases with raising the wavelength to about 800 nm due to decrease and then increases which may be related to the synthesis of CdTe NPs using the sonochemical method. Kenji Okitsu *et al.*, Archan Banerjee *et al.*, and Brajesh Kumar *et al.* have reported similar behavior of Au seeds, TiN, and Ag nanoparticles synthesized by the sonochemical method [51-53].

On the other hand, for the grown layers, a continuous decrease of the extinction coefficient is seen with the increase of the wavelength. The reduction of the extinction coefficient per λ <800 nm for the thin layer, as compared to the synthesized nanoparticles, can be related to the further reduction of light absorption by the film in this infrared region; this indicated the transparency of the film in this region. The refractive index of nanoparticles showed an increasing trend with photon energy due to the density and compactness of the synthesized nanoparticles. The refractive index of the grown films was increased until the photon energy was less than 1.9 eV, which could be due to the matching of the frequency of electromagnetic radiation and electrons in the material [54] before experiencing decrease which indicates a reduction of light reflection in energies more than 1.9 eV. Some of the optical parameters obtained from the light absorption spectrum synthesized by nanoparticles and the grown cadmium telluride films are listed in Table 2.
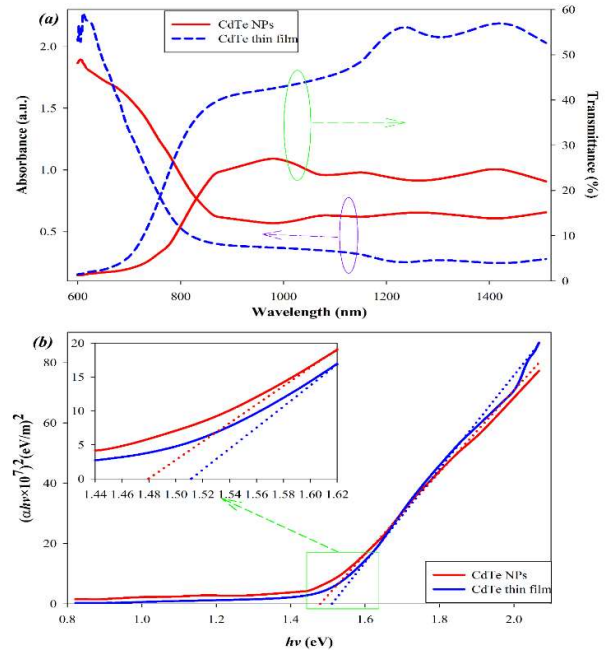


Figure 2. a) Optical spectra of light absorption and transmittance spectrum of nanoparticles and cadmium telluride thin film. b) Tauc diagram of nanoparticles and cadmium telluride thin film in terms of incident photon energy.
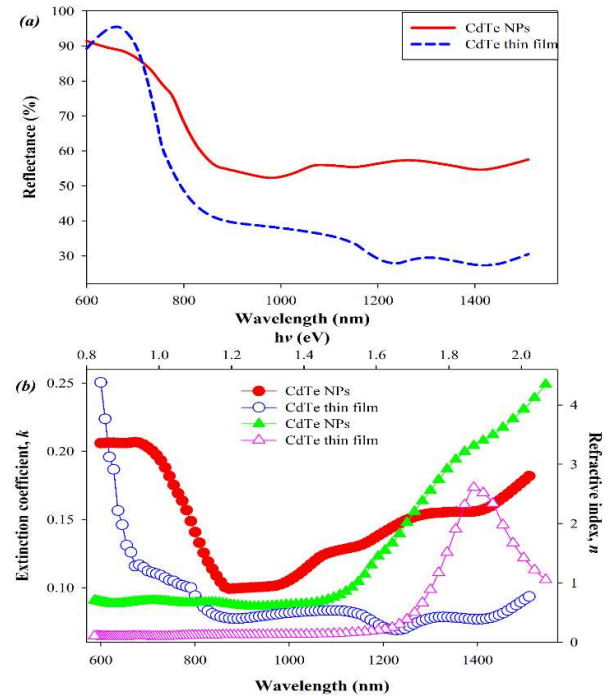


Figure 3. a) Reflectance spectrum of nanoparticles and cadmium telluride thin film. b) Changes in extinction coefficients (●) and refractive index (▲) of nanoparticles and cadmium telluride thin film in terms of wavelength and photon energy, respectively.

Table 2. Some optical and electrical parameters of cadmium telluride at 800 nm.

| *Material* | *Band gap (eV)* | *Extinction Coefficient* | *Refractive Index* |
|---|---|---|---|
| *Nanoparticle* | 1.48 | 0.1407 | 1.0191 |
| *Thin film* | 1.51 | 0.0940 | 0.1667 |

## 3.3 Surface morphology

The surface morphology of the synthesized nanoparticles and the grown films of cadmium telluride is shown in Figure 4; this was according to images taken from the Field Emission Scanning Electron Microscope (FE-SEM). Before imaging, the surface of the material was thoroughly cleaned; to obtain high-resolution images, semiconductor layers such as cadmium telluride were coated with gold nanoparticles, which had a good conductivity to enhance image quality.

High-resolution SEM micrographs showed that the nanoparticles were synthesized uniformly and homogeneity. The distribution of the grown cadmium telluride particles on the substrates was uniform and the surface of the layers did not have any defects such as cracking, cavities and so on. The small size of the particles deposited on the glass confirmed the XRD results. The distance between the nanoparticles accumulated on the substrate was small, as shown, thus indicating that the film was absorbent in the ultraviolet and visible region.
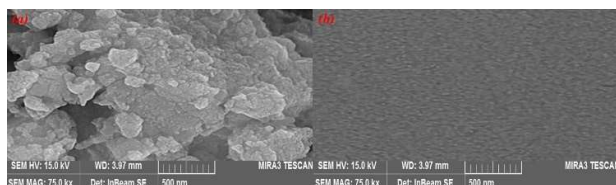


Figure 4. Scanning electron microscope images of field emission: a) Synthesized nanoparticles and b) Thin film of cadmium telluride grown on the glass substrate.

## 4 Conclusions

Cadmium telluride nanoparticles synthesized by the sonochemical method in this work showed different structural properties when compared to nanoparticles produced by the previous methods. One of the most important differences was the change in the preferential orientation of nanoparticles from (111) to (200). The high density and small size of the synthesized nanoparticles could have a great effect on the amount of light absorbed in the material. Use of the thermal evaporation method for deposition and preparation of thin films led to the formation of films with a smaller crystalline size; this was confirmed by the results of the XRD diffraction pattern analysis. Other structural parameters of the synthesized nanoparticles and cadmium telluride thin films on glass, such as microstrain ($\varepsilon$), dislocation density ($\delta$), and tissue coefficient ($T_C$) have been investigated by X-ray diffraction patterns. The texture coefficient of the grown films showed that the preferential orientation (200) did not change after deposition, but the peak intensity related to this direction was reduced. The optical properties of the synthesized nanoparticles and the prepared films showed that the nanoparticles synthesized by sonochemistry had a higher absorption value in the ultraviolet-visible region.

After deposition, the films grown in the infrared region became completely transparent; the energy band gap obtained for the nanoparticles and films was in a good agreement with the previous studies. Scanning electron microscopy images also showed that the sonochemical method produced nanoparticles with uniformity and homogeneity. Examination of the morphology of the grown layers also confirmed the uniformity and homogeneity of the surface of the grown thin film. The results obtained in this work, thus, showed the synthesis of a new type of cadmium telluride semiconductor (200) that had desirable structural and optical properties for various applications, including the development of electro-optical devices such as solar cells.

## References

[1] K. Ogawa et al., "Development of an ultra-high resolution SPECT system with CdTe semiconductor detector." Annals of Nuclear Medicine, **23** (2009) 763.

[2] R. M. Amin et al., "Fluorescence-based CdTe nanosensor for sensitive detection of cytochrome C." Biosensors and Bioelectronics **98** (2017) 415.

[3] C. Liu et al., "Visible-light driven photocatalyst of CdTe/CdS homologous heterojunction on N-

rGO photocatalyst for efficient degradation of 2, 4-dichlorophenol." Journal of Taiwan Institute of Chemical Engineers, **93** (2018) 603.

[4] G. Yang et al., "Photosensitive cadmium telluride thin-film field-effect transistors." Optics Express, **24** (2016) 3607.

[5] W. Chen et al., "Voltage tunable electroluminescence of CdTe nanoparticle light-emitting diodes." Journal of Nanoscience and Nanotechnology, **2** (2002) 47.

[6] M. Hädrich et al, "Formation of CdSxTe1-x at the p-n junction of CdS-CdTe solar cells." Physica Status Solidi (C) Current Topics in Solid State Physics, **6** (2009) 1257.

[7] E. Hasani and D. Raoufi, "Influence of temperature and pressure on CdTe:Ag thin film." Surface and Engineering, **34** (2018) 914.

[8] M. Sh. Hossain et al, " Impact of CdTe thin film thickness in ZnxCd1-xS/CdTe solar cell by RF sputtering." Solar Energy, **180** (2019) 559.

[9] K. S. Rahman et al, "Influence of deposition time in CdTe thin film properties grown by close-spaced sublimation (CSS) for photovoltaic application." Results in Physics, **14** (2019) 102371.

[10] J. P. Enriquez and X. Mathew, "XRD study of the grain growth in CdTe films annealed at different temperatures." Solar Energy Materials and Solar Cells, **81** (2004) 363.

[11] M. F. Al-Kuhaili et al., "Influence of vacuum annealing on the photoresponse of thermally evaporated cadmium telluride thin films." Thin Solid Films, **686** (2019) 137412.

[12] L. Feng et al., "The electrical, optical properties of CdTe polycrystalline thin films deposited under Ar-O2 mixture atmosphere by close-spaced sublimation." Thin Solid Films, **491** (2005) 104.

[13] M. A. Green et al., "Solar cell efficiency tables (Version 52)." Progress in photovoltaics: Research and applications, **26** (2018) 427.

[14] T. Takahashi and S. Watanabe, "Recent progress in CdTe and CdZnTe detectors." IEEE Transaction on Nuclear Science, **48** (2001) 950.

[15] E. Hasani et al, "Synthesis and deposition of (200)-oriented CdTe thin films on transparent substrates." Materials Research Express, **6** (2019) 046422.

[16] I. Ban et al, "Preparation of cadmium telluride nanoparticles from aqueous solutions by sonochemical method." Materials Letters, **67** (2012) 56.

[17] J. Ling et al., "Electrodeposition of CdTe thin films for solar energy water splitting." Materials **13** (2020) 1536.

[18] I. R. Agool et al., "Synthesis and characterization of CdTe NPs induced by laser ablation in liquid." Journal of Advanced Physics, **6** (2017) 241.

[19] K. S. Suslick et al., "Sonochemical synthesis of amorphous iron." Nature, **353** (1991) 414.

[20] D. Chen et al., "Handbook on Applications of ultrasound: sonochemistry for sustainability." CRC Press, 2011.

[21] A. Umer et al., "Selection of a suitable method for the synthesis of copper nanoparticles." Nano, **07** (2012) 1230005.

[22] P. Bartolo-Pérez et al., "X-Rey photoelectron spectroscopy study of CdTe oxide films grown by rf sputtering with an Ar-NH3 plasma." Surface and Coatings Thechnology, **155** (2002) 16.

[23] J. Ramiro et al., "Pulsed laser deposition and electrodeposition techniques in growing CdTe and CdxHg1-xTe thin films." Thin Solid Films **361-362** (2000) 65.

[24] V. V. Brus et al, "Graphitic Carbon/n-CdTe schottky-type heterojunction solar cells prepared by electron-beam evaporation." Solar Energy, **112** (2015) 78-84.

[25] D. Verma et al, "Surfactant-free CdTe nanoparticles mixed MEH-PPV hybrid solar cell deposited by spin coating technique." Solar Energy Materials and Solar Cells, **93** (2009)

1482.

[26] X. Wen et al., "Epitaxial CdTe thin films on mica by vapor transport deposition for flexible solar cells." ACS Applied Energy Materials, **3** (2020) 4589.

[27] Z. Mahmoud Nassar et al., "Structural and optical properties of CdTe thin film: A detailed investigation using optical absorption, XRD, and Raman spectroscopies." Physica Status Solidi (b) Basic Solid State Physics, **253** (2016) 1104.

[28] E. Hasani et al, "Effect of high-pressure annealing on the physical properties of the CdTe thin films." The European physical journal plus, **136** (2021) 1.

[29] S. Chander and M. S. Dhaka, "CdCl₂ treatment concentration evolution of physical properties correlation with surface morphology of CdTe thin films for solar cells." Materials Research Bulletin, **97** (2018) 128.

[30] A. Escobedo et al., "Characterization of smooth CdTe (111) films by thee conventional close-spaced sublimation technique." Journal of Electronic Materials, **39** (2010) 400.

[31] H. I. Salim et al., "Electrodeposition of CdTe thin films using nitrate precursor for applications in solar cells." Journal of Materials Science: Materials in Electronics, **26** (2015) 3119.

[32] Y. Gu et al., "Influence of surface structures on quality of CdTe(100) thin films grown on GaAs(100) substrates." Chinese Physics Letters, **35** (2018) 086801.

[33] Sh. X. Zhang et al., "Characterization of the microstructures and optical properties of CdTe(001) and (111) thin films grown on GaAs(001) substrates by molecular beam epitaxy." Journal of Crystal growth, **546** (2020) 125756.

[34] J. P. Faurie et al., "CdTe-GaAs(100) interface: MBE growth, rheed and XPS characterization." Surface Scince, **168** (1986) 473.

[35] L. A. Kolodziejski and R. L. Gunshor "Epitaxial growth of CdTe on GaAs by molecular beam epitaxy." Journal of Vacuum science & technology A, **4** (1986) 2150.

[36] E. Campos-González et al, "Structural and optical properties of CdTe-nanocrystals thin films grown by chemical synthesis." Materials Science in Semiconductor Processing, **35** (2015) 144.

[37] F. Hosseinpanahi et al, "Fractal feature of CdTe thin films grown by RF magnetron sputtering", Applied Surface Science 357 (2015) 1843.

[38] A. L. Patterson, "The Scherrer formula for X-ray particle size determination." Physical Review, **56** (1939) 978.

[39] G. K. Williamson and W. H. Hall, "X-ray line broadening from field aluminum and wolfram." Acta Metallurgica, **1** (1953) 22.

[40] G. K. Williamson and R. E. Smallman, "III. Dislocation densities in some annealed and cold-worked metals from measurements on the X-ray debye-Scherrer spectrum." The Philosophical Magazine: A Journal of Theoretical Experimental and Applied Physics, **1** (1956) 34.

[41] G. B. Harris, "X. Quantitative measurement of preferred orientation in rolled uranium bars." The London, Edinburgh and Dublin Philosophical Magazine and Journal of Science, **43** (1952) 113.

[42] H. R. Moutinho et al., "Investigation pf polycrystalline CdTe thin films deposited by physical vapor deposition, close-spaced sublimation and sputtering." Journal of Vacuum Science & Technology A, **13** (1995) 2877.

[43] A. L. Rogach, "Nanocrystalline CdTe and CdTe(S) particles: wet chemical preparation, size-dependent optical properties and perspectives of optoelectronic applications." Material Science and Engineering B, **69-70** (2000) 435.

[44] J. Polit et al., "High resolution spectra of defects in CdTe obtained in Far-infrared region using synchrotron radiation." Infrared Physics & Technology, **49** (2006) 23.

[45] J. Tauc, "Optical properties and electronic structure of amorphous Ge and Si." Materials Research Bulletin, **3** (1968) 37.

[46] H. Abitan et al., "Correction to the Beer-Lambert-Bouguer law for optical absorption." Applied Optics, **47** (2008) 5354.

[47] E. Hasani et al., "Study of structural, electrical and optical properties of (200)-oriented CdTe thin films depending on the post-deposition low temperature." Journal of Electronic Materials, **49** (2020) 4134.

[48] J. Novák et al., "Influence of tensile and compressive strain on the band gap energy of ordered InGaP." Applied Physics Letters, **79** (2001) 2758.

[49] S. Sanjeev and D. Kekuda, "Effect of annealing temperature on the structural and optical properties of zinc oxide (ZnO) thin films prepared by spin coating process." IOP Conference Series: Materials Science and Engineering, **73** (2015) 012149.

[50] W. W. Yu et al., "Experimental determination of the extinction coefficient of CdTe, CdS nanocrystals." Chemistry of Materials, **15** (2003) 2854.

[51] K. Okitsu and S. Semboshi, "Synthesis of Au nanorods via autocatalytic growth of Au seeds formed by sonochemical reduction of Au(I): Relation between formation rate and characteristics of Au nanorods." Ultrasonics Sonochemistry, **69** (2020) 105229.

[52] A. Banerjee et al., "Optical properties of refractory metal based thin films." Optcal Materials Express, **8** (2018) 2072.

[53] B. Kumar et al., "Sonochemical synthesis of silver nanoparticles using starch: A comparison." Bioinorganic Chemistry and applications, **2014** (2014) 784268.

[54] K. Punitha et al., "Physical properties of electron beam evaporated CdTe and CdTe:Cu thin films." Journal of Applied Physics, **116** (2014) 213502.